TRACE SPACE RECONSTRUCTION FROM PEPPERPOT DATA

H.R. Kremers*, J.P.M. Beijers, V. Mironov, J.Mulder, S. Saminathan, S. Brandenburg,
Kernfysisch Versneller Instituut, Groningen, The Netherlands

Abstract

In this paper we present a simple model that we developed to reconstruct the 4D trace space distribution from the convoluted spatial images of a pepperpot emittance meter. Straightforward analysis of the images is hampered because of multiple and/or overlapping beamlets emerging from a single hole in the pepper plate. The model allows us to unambiguously assign each transmitted beamlet to its corresponding hole in the pepper plate from which it emerged. We will illustrate our analysis model with the reconstruction of the 4D trace space distribution behind the analyzing magnet of a He^{1+} beam extracted from an electron cyclotron resonance ion source.

INTRODUCTION

It is well known that electron cyclotron resonance ion sources (ECRIS) produce ion beams with relatively large emittances, i.e. several tens of π mm-mrad or even larger. Such low-quality ion beams are difficult to transport to and inject into an accelerator with high efficiency. Much work is therefore being devoted to better understand and improve low-energy ion beam transport. At KVI we made some progress by a combined effort of detailed beam transport simulations and measurements of beam profiles and emittances. This is reported in an accompanying paper to these proceedings [1]. To measure the 4D beam emittance of low-energy multiply-charged ion beams we built a pepperpot emittance meter and installed it in the image plane of the analyzing magnet [2]. However, overlapping and multiple beamlets emerging from a single hole in the pepper plate complicate a straightforward reconstruction of the 4D trace-space of the ion beam. This paper presents a simple method that we developed to overcome this problem. After a brief description of the emittance meter the above-mentioned problem will be illustrated with an emittance measurement of a 21 keV He^{1+} beam. Then the analysis method will be outlined that we developed to unambiguously reconstruct the 4D trace-space distribution of the ion beam.

PEPPERPOT EMITTANCE METER

The KVI4D emittance meter combines the pepperpot and scanning techniques to measure the 4D trace-space distribution of ion beams which have a large divergence and narrow width in the horizontal plane and a small divergence and large width in the vertical plane [2]. This is done by stepping a pepper plate with a linear array of holes aligned in the vertical direction horizontally through the beam and measuring the images of the transmitted beamlets at each step with a position-sensitive detector positioned 59 mm downstream of the pepper plate. The pepper plate is a 25 μm tantalum foil, mounted on a water-cooled copper block, with a vertical row of 20 holes each with a diameter of 20 μm and a pitch of 2 mm. The step width in the horizontal direction depends on the desired resolution, and is typically around 0.5 mm. We installed the pepperpot emittance meter near the focal plane of the 110° analyzing magnet.

An emittance measurement consists of measuring a series of spatial images of the transmitted beamlets, one at each horizontal step. As an example we measured the emittance of a 21 keV He^{1+} beam. The horizontal step size was set at 0.56 mm and we measured 39 spatial images of the transmitted beamlets from which the 4D trace-space distribution has to be reconstructed. A single spatial image taken at the horizontal position of x=-4 mm is shown in Fig. 1a. Also the location of the holes in the pepper plate is indicated. Fig. 1a clearly shows that there are i) more beamlets than there are holes and ii) some of the beamlets are overlapping. This complicates the analysis.

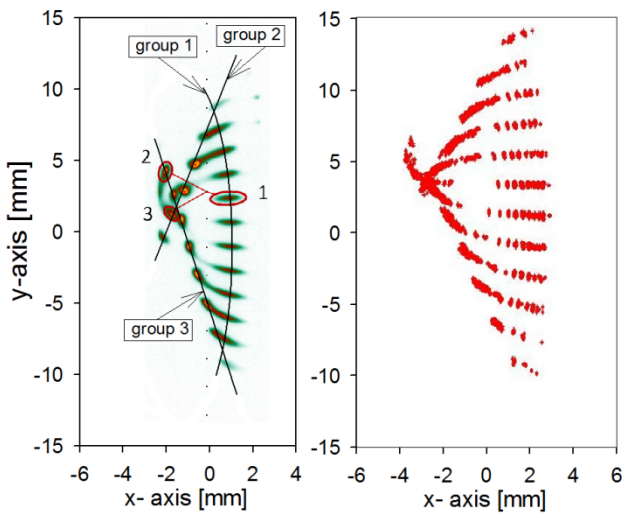

Figure 1: Measured a) and simulated b) spatial image obtained with the KVI4D emittance meter of transmitted beamlets with the pepper plate positioned at x=-4 mm for a 21 keV He^{1+} beam.

THE ANALYSIS

As already mentioned above the measured spatial images sometimes show both overlapping beamlets and, particularly around the median plane, multiple beamlets emerging from a single hole. From the systematic trend in the series of 39 images we could connect each beamlet with the hole in the pepper plate from which it emerged. An example is shown in Fig. 1a where three beamlets are connected that emerge from one hole. In addition, it

* kremers@kvi.nl

appeared convenient to classify all the beamlets into three groups with identical behavior. These are also indicated in Fig. 1a. In order to check our assignments we performed a detailed simulation of the beam transport from the ECRIS plasma electrode through the analyzing magnet to the scintillation screen of the emittance meter. The simulation method is described in more detail in Ref. [1]. The simulation result is shown in Fig. 1b and confirmed our initial assignments. Although 10^6 particles were used in the simulation, the calculated image has a much more granular appearance than the measured one. This is caused by the fact that the pepper plate intercepts most of the particles. The simulation also showed that the beamlets belonging to group 1 follow the more paraxial trajectories through the analyzing magnet, while the group 2 and 3 beamlets make a relatively large vertical angle (either positive or negative) with the median plane.

In order to reconstruct the 4D trace-space distribution we have to disentangle the overlapping beamlets. This was done by using an ellipse fitting routine to determine the center coordinates (x_c^i, y_c^i) of every beam spot in the plane of the scintillation detector, with the label i denoting the group to which each spot belongs. Next we fitted the center coordinates with a two-dimensional second-order polynomial according to:

$$x_c^i = \sum_{m,n=0}^{2} a_{mn}^i x_s^m y_s^n \; ; \; y_c^i = \sum_{m,n=0}^{2} b_{mn}^i x_s^m y_s^n \qquad (1)$$

with (x_s, y_s) the coordinates in the scintillation plane. The fit results in 18 coefficients for one group, i.e. 9 coefficients for x_c^i and 9 for y_c^i. Knowing the center coordinates of all the beam spots and the center coordinates of the holes in the pepper plate to which they belong, it is straightforward to reconstruct the 4D trace-space density $\rho(x,y,x',y') = \Sigma_i \rho^i(x,y,x',y')$ of the ion beam. Here, (x,y) are the center coordinates of the holes in the pepper plate and $x' = (x_s - x)/L$, $y' = (y_s - y)/L$ and L = 59 mm the distance between the scintillation screen and the pepper plate.

TRACE-SPACE DISTRIBUTIONS

From the 4D trace-space distribution $\rho(x,y,x',y')$ we can calculate various 2D projections by integrating over the two other coordinates. For example, the 2D spatial distribution $\rho(x,y)$ is obtained from $\rho(x,y,x',y')$ by calculating

$$\rho(x,y) = \iint \rho(x,y,x',y')dx'dy'. \qquad (2)$$

This is illustrated in Fig. 2 for the He^{1+} beam showing the groups i=1, i=2,3, all three groups and the simulated spatial profile. The spatial profiles show a strong second-order aberration which we attribute to the analyzing magnet [1].

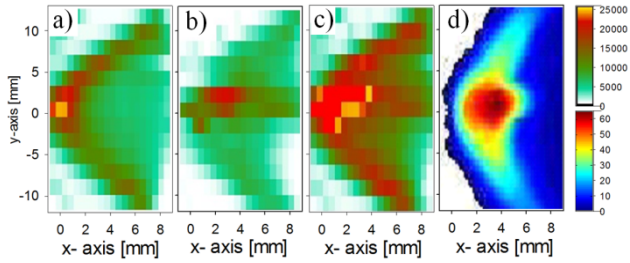

Figure 2: Spatial distribution of a 21 keV He^{1+} beam behind the analyzing magnet. a) group 1 ions; b) group 2,3 ions; c) all ions; d) simulated 2D profile.

For the horizontal trace-space distribution $\rho(x,x')$ (x-x' emittance) we get

$$\rho(x,x') = \iint \rho(x,y,x',y')dydy'. \qquad (3)$$

This is shown in Fig. 3 for the different ion groups together with a simulated emittance distribution. Both the measured and simulated x-x' trace-space distributions show a diverging beam, although the simulated distribution is less diverging than the measured one. Interestingly, the ions in group 2 and 3 have a relatively large negative offset in angle, i.e. their deflection angles are less than 110°. We will investigate this further in the next section.

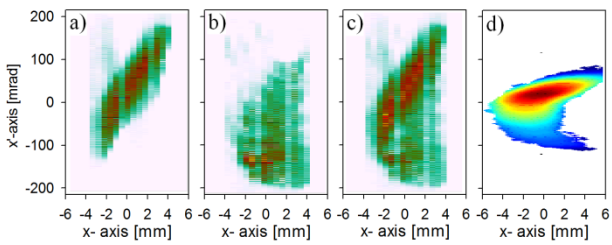

Figure 3: Horizontal x-x' emittance distribution of a 21 keV He^{1+} beam behind the analyzing magnet. a) group 1 ions; b) group 2,3 ions; c) all ions; d) simulated x-x' emittance distribution.

The vertical trace-space distribution $\rho(y,y')$ (y-y' emittance) is given by

$$\rho(y,y') = \iint \rho(x,y,x',y')dxdx'. \qquad (4)$$

Fig. 4 shows some of the vertical emittance distributions summed over all three ion groups. In Fig. 4a a partial vertical emittance is plotted, i.e. measured at the horizontal position x = 5.6 mm. This figure clearly shows that from the holes close to the median plane y = 0 three different beamlets emerge, i.e. one with a very small vertical angle and two with larger positive and negative vertical angles. The S-shape suggests a third-order aberration, which is probably caused by the pole face rotation of the analyzing magnet. Figs. 4b and c show the measured and simulated vertical emittances summed over all three ion groups, respectively. The characteristic

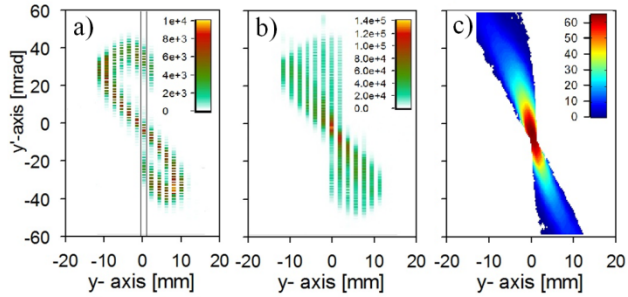

Figure 4: Vertical y-y' emittance distributions of a 21 keV He^{1+} beam behind the analyzing magnet summed over all three ion groups. a) y-y' emittance at the horizontal position x = 5.6 mm; b) total y-y' emittance; c) simulated y-y' emittance distribution.

bowtie shape of the y-y' emittance results from integration over the x coordinate.

BACKTRANSFORMATION

In order to investigate the horizontal imaging properties of the analyzing magnet further we constructed its transfer map T up to second order from the ion trajectory calculations described in Ref.[1]. The transfer map T projects a trace-space vector x(0) at the end of the ground electrode of the ECRIS extraction system to its corresponding vector x(1) in the image plane of the analyzing magnet. Using the inverse map T^{-1} we then projected each 4D point x(1) back to its corresponding point x(0), i.e. $x(0)=T^{-1}x(1)$, and from this we have calculated the 4D trace-space distribution $\rho^0(x,y,x',y')$ of the ions at the end of the ground electrode.

As an example we show in figure 5 the spatial distributions of the ions projected back from the image plane of the analyzing magnet to the end of the ground electrode before the magnet. Plotted are the spatial distributions of the group 1 ions, the ions of groups 2 and 3 and of all ions. The figure confirms that group 1 ions follow more or less paraxial trajectories. Ions belonging to groups 2 and 3 on the other hand are offset in both x and y coordinates with respect to the group 1 ions. Their starting positions are horizontally shifted to the inward side of the analyzing magnet and are vertically shifted above and below the median plane. The ions belonging to groups 2 and 3 follow trajectories that probe the fringe field of the analyzing magnet more than the group 1 ions do and are therefore deflected less.

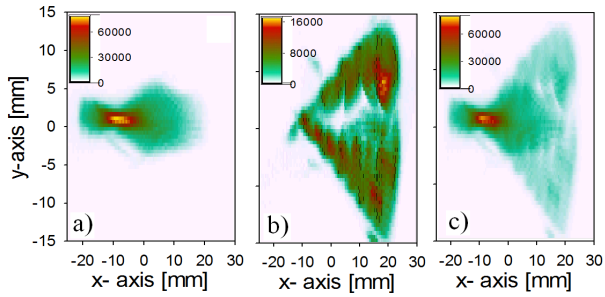

Figure 5: Back transformed spatial distributions of 21 keV He^{1+} ions at the end of the ground electrode before the analyzing magnet calculated from the measured trace-space distribution in the image plane of the magnet. a) group 1 ions; b) group 2,3 ions; c) all ions.

CONCLUSIONS

We have developed a method which allows us to reconstruct the 4D trace-space distribution of a low-energy ion beam from measured spatial images of a pepperpot emittance meter in the presence of multiple and overlapping beam spots. The method is illustrated with a detailed analysis of the 4D trace-space distribution of a 21 keV He^{1+} beam measured in the image plane of the analyzing magnet. We find that in our case the measured trace-space distributions are to a large extent determined by the ion-optical properties of the analyzing magnet. The measured trace-space distributions agree reasonably well with detailed beam transport simulations.

REFERENCES

[1] S. Saminathan et al., these proceedings.
[2] H.R. Kremers, J.P.M. Beijers, S. Brandenburg, DIPAC07 Proc. Triëste, p. 169-171, 2007.

Trace space reconstruction of pepperpot data

H.R. Kremers

Kernfysisch Versneller Instituut

Content

- AECR source setup.
- KVI4D pepper pot emittance meter.
- Trace space measurement.
- Analysis (reconstruction)
- Results (projections)
- Conclusions.

AECR ion source setup

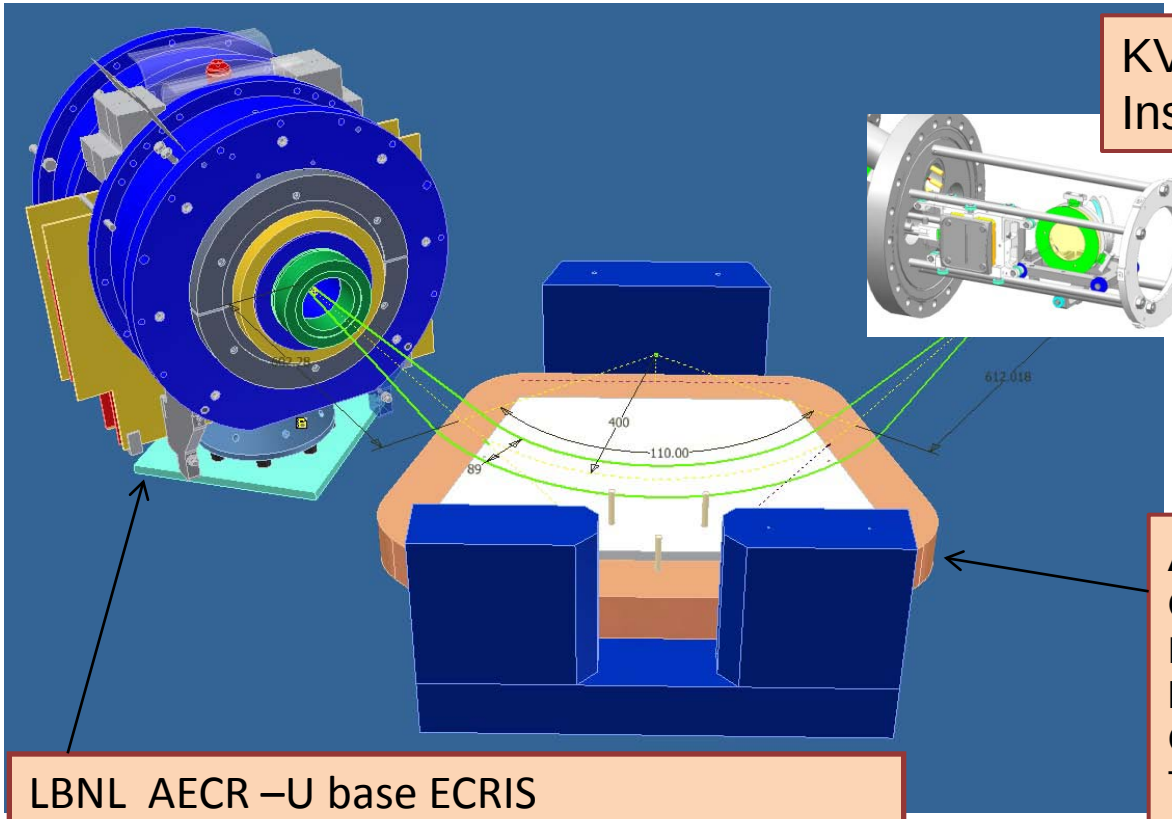

KVI4D emittance meter
Installed in image plane

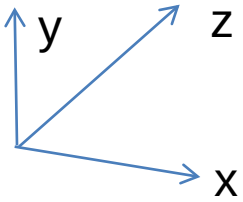

Analyzing magnet

Θ_{bend} = 110 degrees
R_{bend} = 40 cm
$B_{pole\ face\ rot}$ = 37 deg
Gap = 67 mm
Transport eff = 70%
no clamping
Pole Shape: straight edge

LBNL AECR –U base ECRIS

- V_{ext} max= 35 kV
- RF 14 Ghz(1.1 kW), TwT 11-12.5 GHz(400W)
- B_{inj}=2.1T, B_{ex}=1.1T, B_{rad}=0.9T
- Pressure 5.10^{-8}-2.10^{-7} mbar.

Typical beam currents:

$^{204}Pb^{27+}$: 25 eμA
$^{16}O^{4+}$: 500 eμA

KVI4D pepper pot emittance meter

Pepper pot plate (array 20 x ø20 micron holes)

Multi channel plate detector

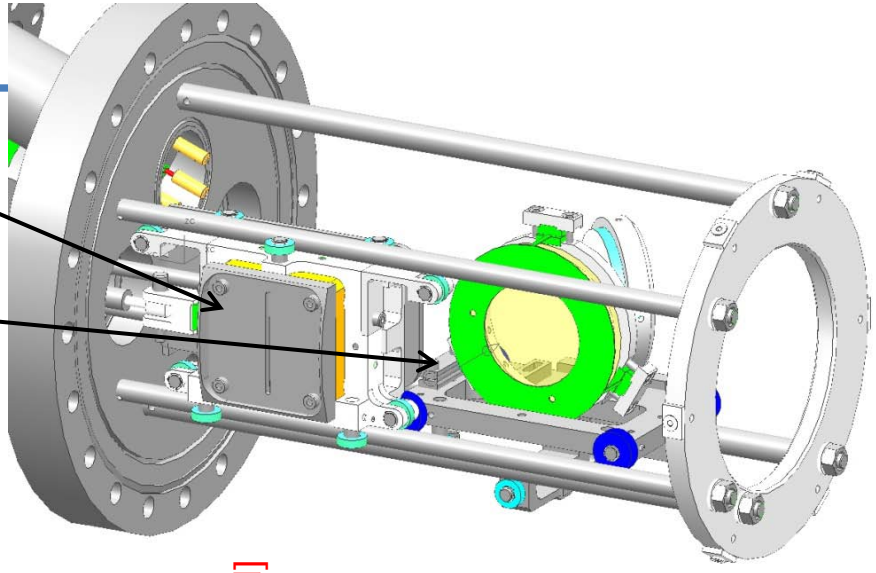

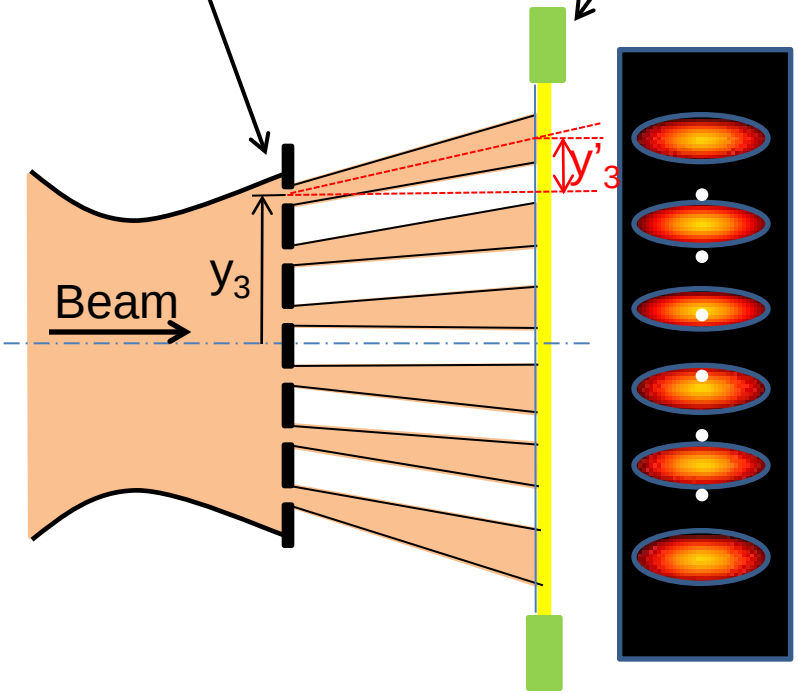

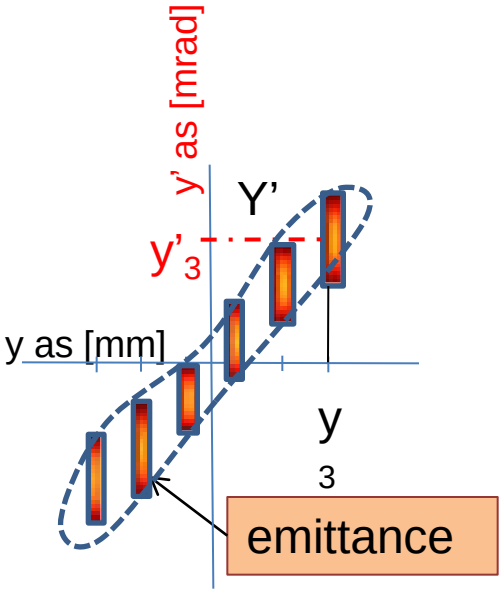

Trace space of a 21 keV He^{1+} beam

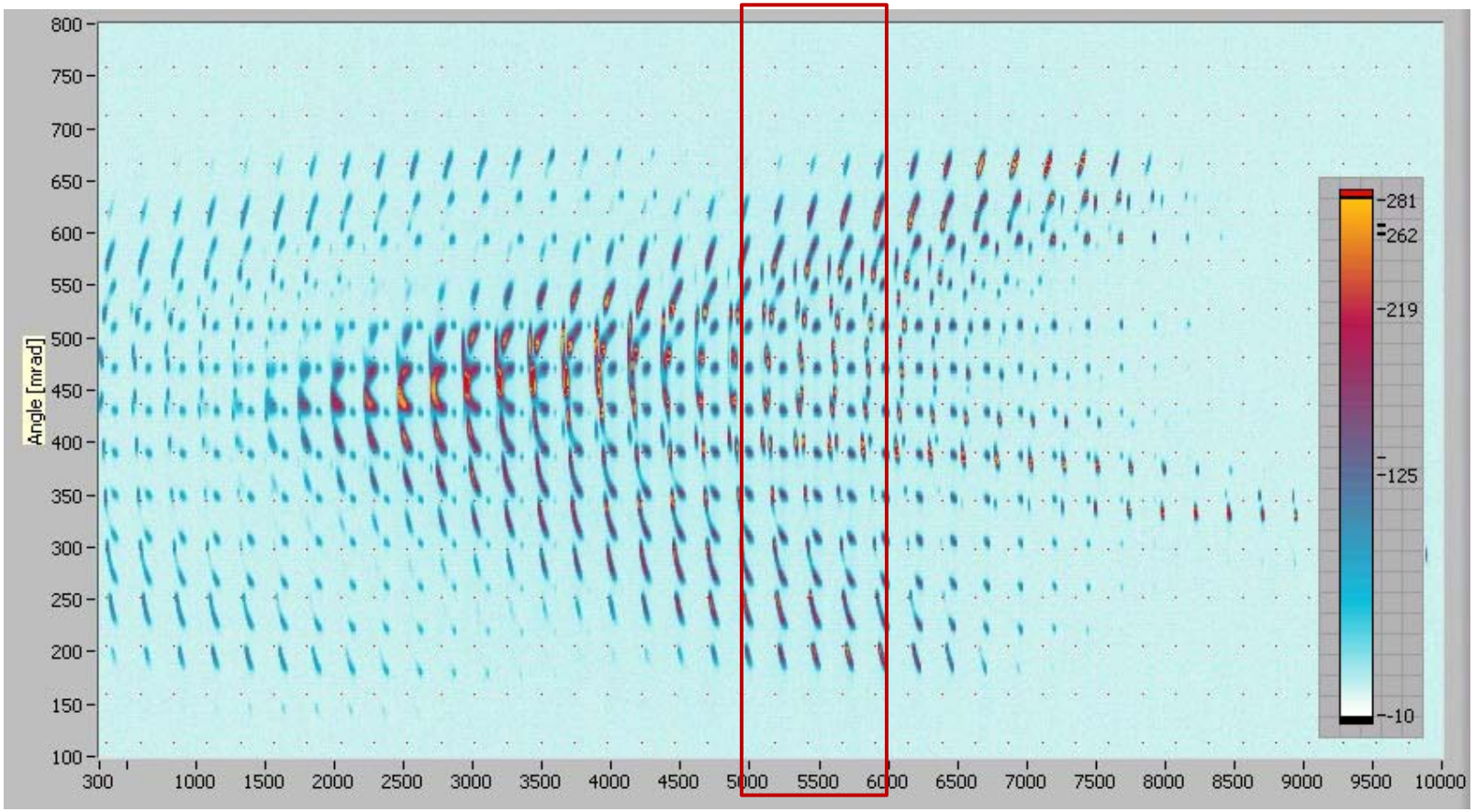

Response distribution of array of 20 holes

on four positions in the beam

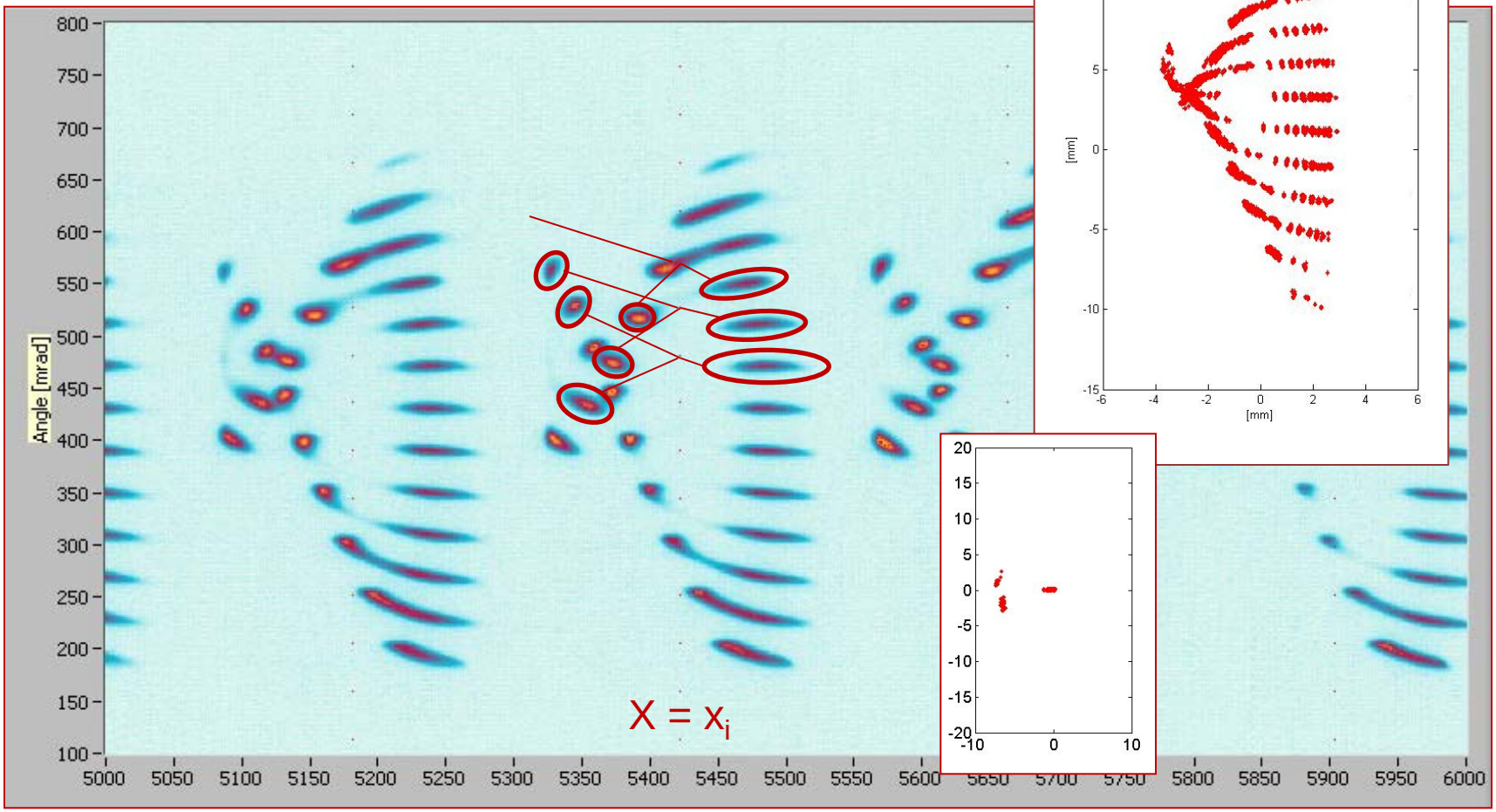

Overlap of response distributions

Beside: x, y , x', y
- group identity' i=1,2 or3

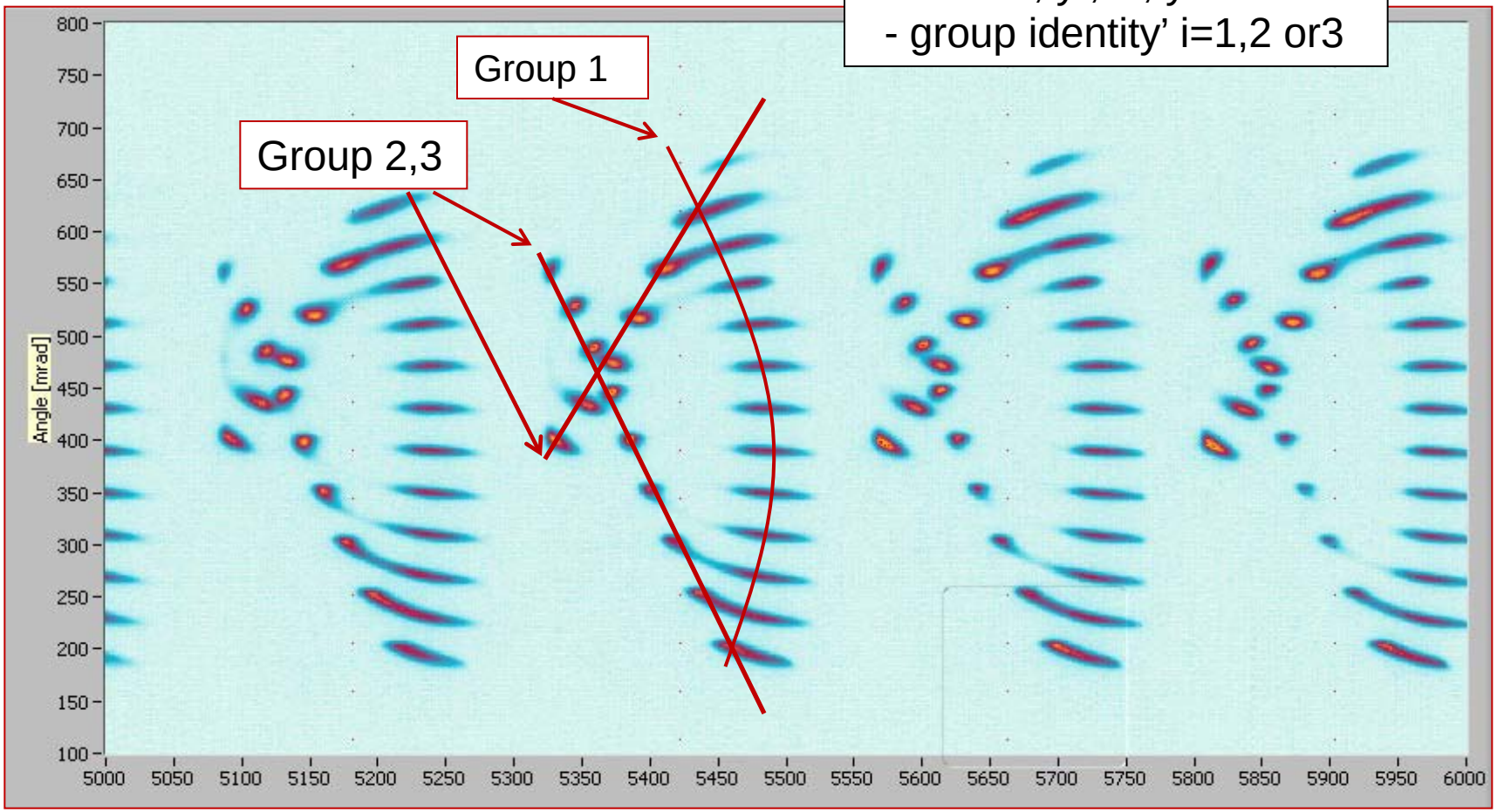

Data modeling.

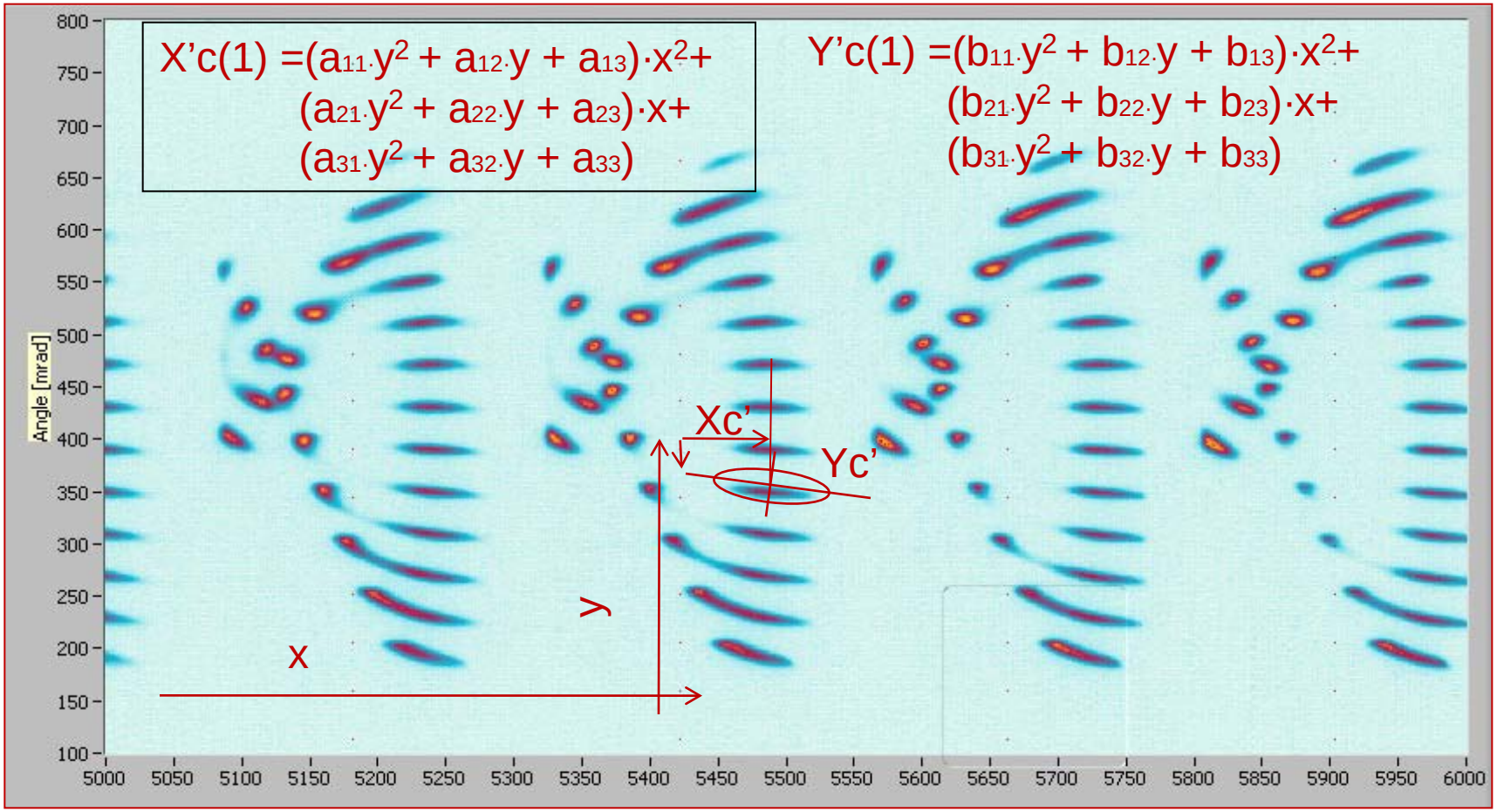

The four dimensional dataset

$$\mathrm{P}_i = \rho\left(x, y, x', y'\right)_i$$

- Dataset is unambiguous
  - Extra label (i) for group 1,2 or 3.

- Projections in the image plane as function of (i).
  x-y projection known as viewing screen
  x-x'projection used for a x-x'emittance
  y-y'projection used for a y-y'emittance
  x'-y'projection

Result of the model

x-y projection. (viewing screen projection)

$$P(x,y)_{i=1} = \int_{y'=-20mrad}^{y'=+20mrad} \int_{x'=-60mrad}^{x'=+60mrad} \rho(x,y,x',y')_1 dx'\,dy'$$

i =1

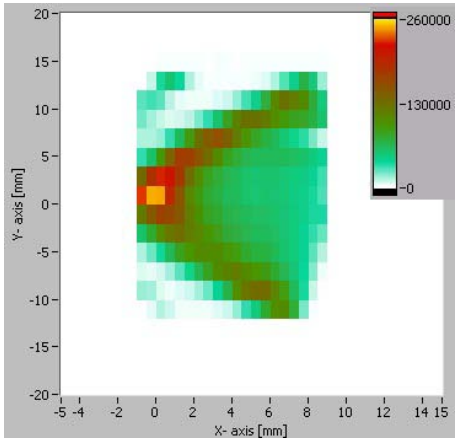

i=2,3

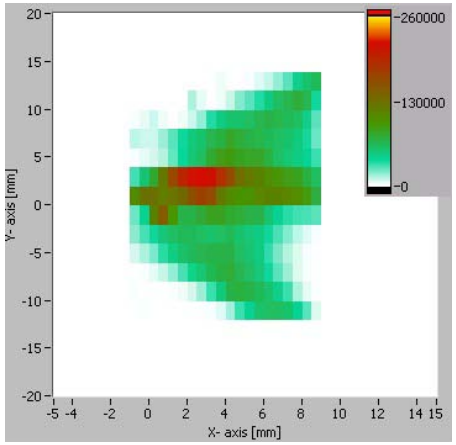

i=1,2 and 3

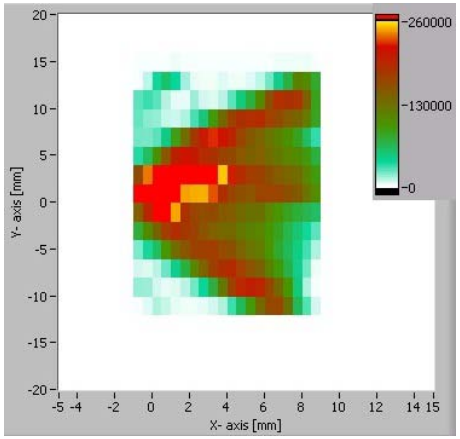

camera recording

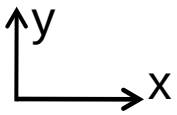

The emittances in the image plane

y-y’ projection

$$P_i(y,y') = \int_{x=-12mm\ x'=-60mrad}^{x=+12mm\ x'=+60mrad} \rho(x,y,x',y')_i dx dx'$$

2 sigma 320 π mm mrad

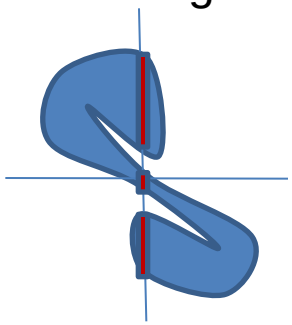

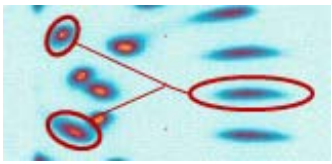

group 1

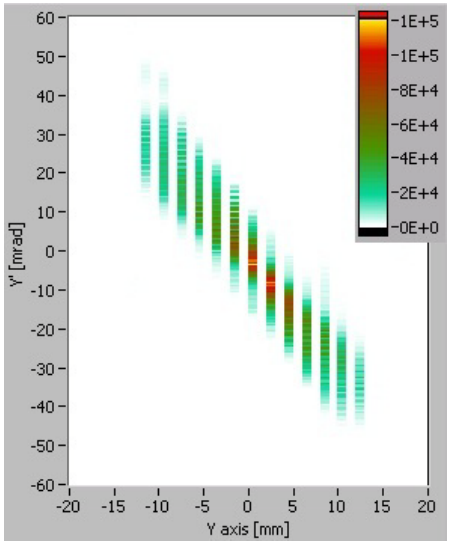

group 2,3

group2

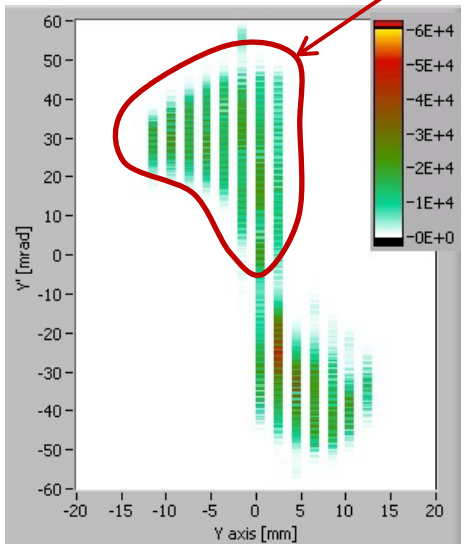

group 1,2,3

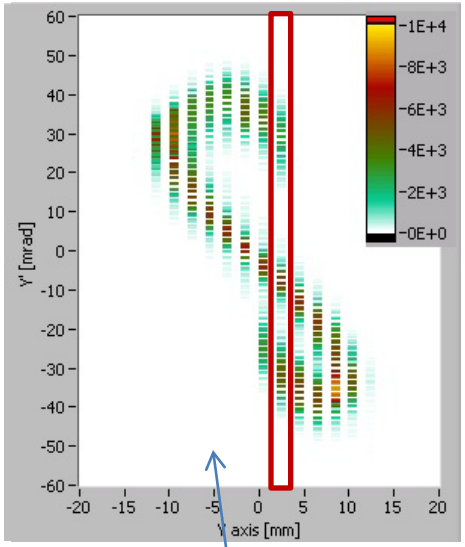

y-y’for only one x position: x=-10

Transformation to object plane in 2de orde

$$[P_i]_{image\cdot plane} = [\rho(x, x', y, y')_i]_{image\cdot plane}$$

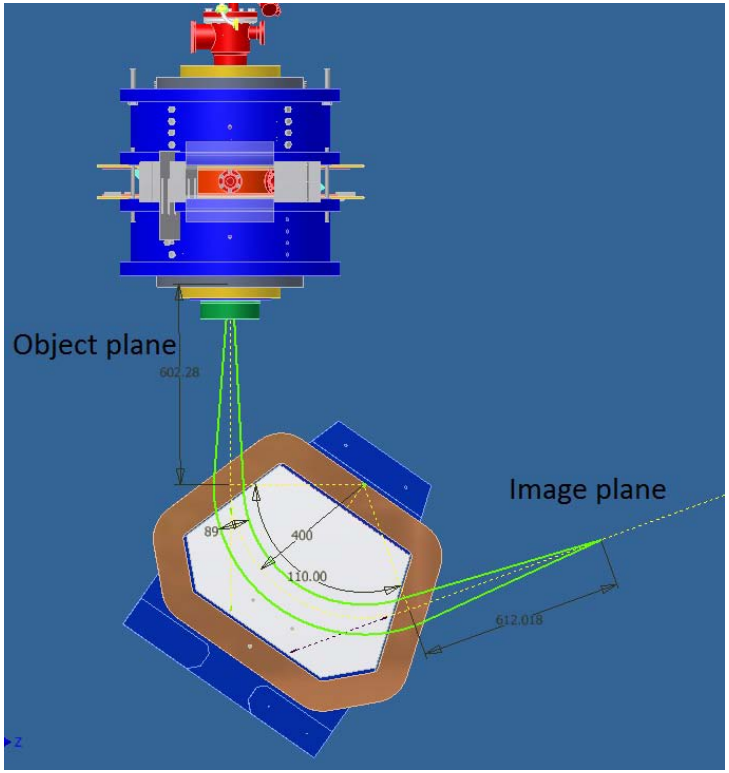

$$P_{im} = M^{2^{de}} \cdot P_{obj} \rightarrow P_{obj} = M^{2^{de}\ -1} \cdot P_{im}$$

Transformation to entrance of M110 of x-y projections (viewing screen projections)

group 1

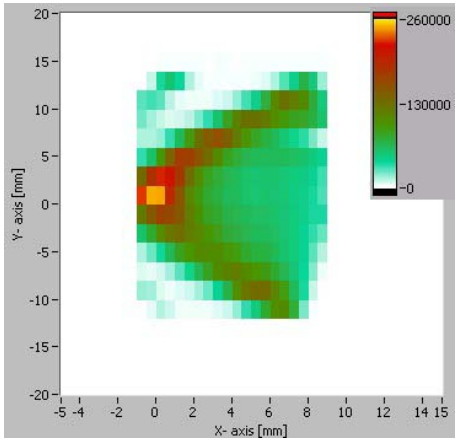

group 2,3

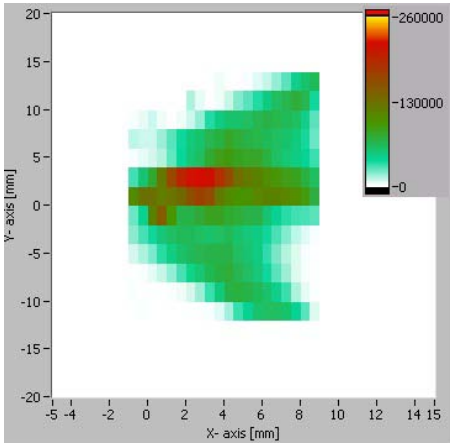

group 1,2,3

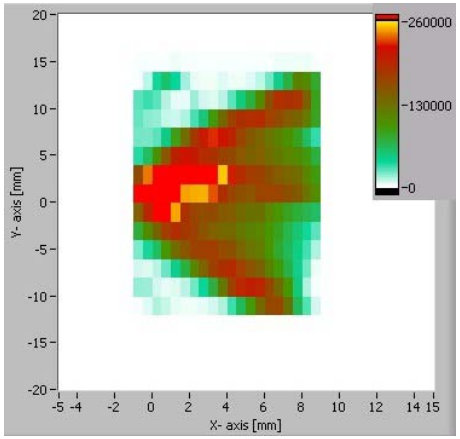

$X_f = M \cdot X_o$

$X_o = M^{-1} \cdot X_f$

In image plane

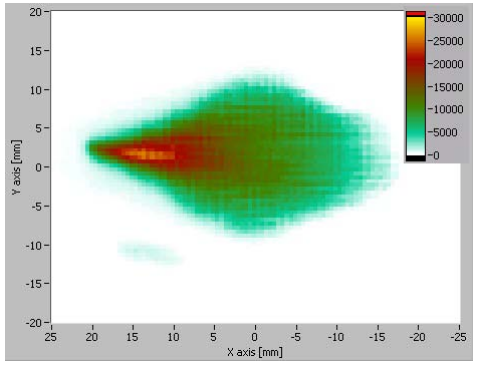

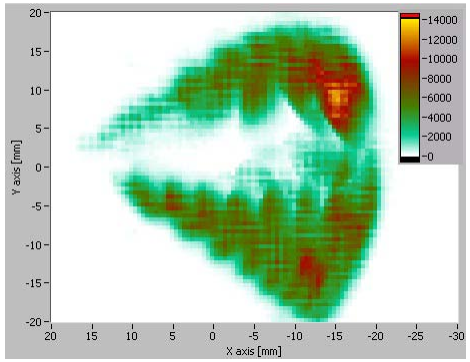

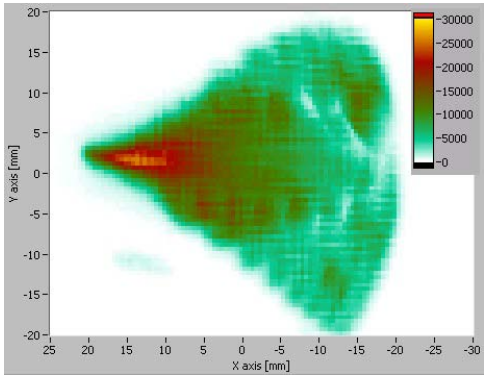

In object plane

rijksuniversiteit groningen

KVI

Conclusions:

- Dipole induced second order aberration of the beam.
- Group 2,3 created by the dipole fringe field
- Three beams can emerge due to S-shape emittance in y-y'phase-space.
- These Trace-space patterns are not plasma related effects
- Plasma-related effects can be seen at the entrance of the analyzing magnet as a non homogeneous distribution.

Future outlook

- Installation of a new analyzing magnet
  - Compensation for the second order aberration
  - Gap increase with a factor of 2.
- New emittance meter KVI4D-advanced is in construction to operate at G.S.I. (ready feb2011)

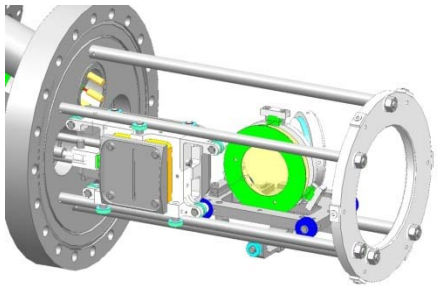

KVI4D

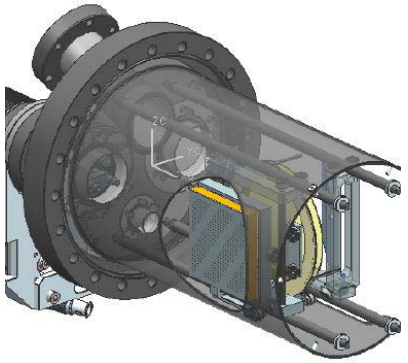

KVI4D-ADV

KVI ion source group

- KVI Ion source group
  - Sytze Brandenburg
  - Hans Beijers
  - Vladimir Mironov
  - Suresh Saminathan
  - Jan Mulder
  - Rob Kremers

Thank you for your attention

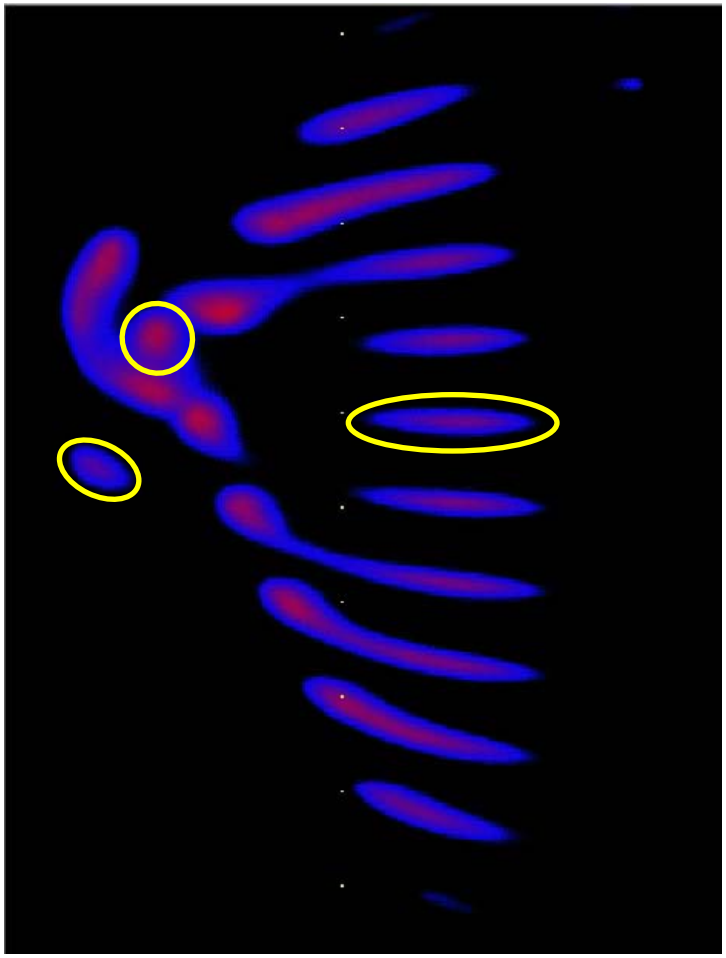

Trace space

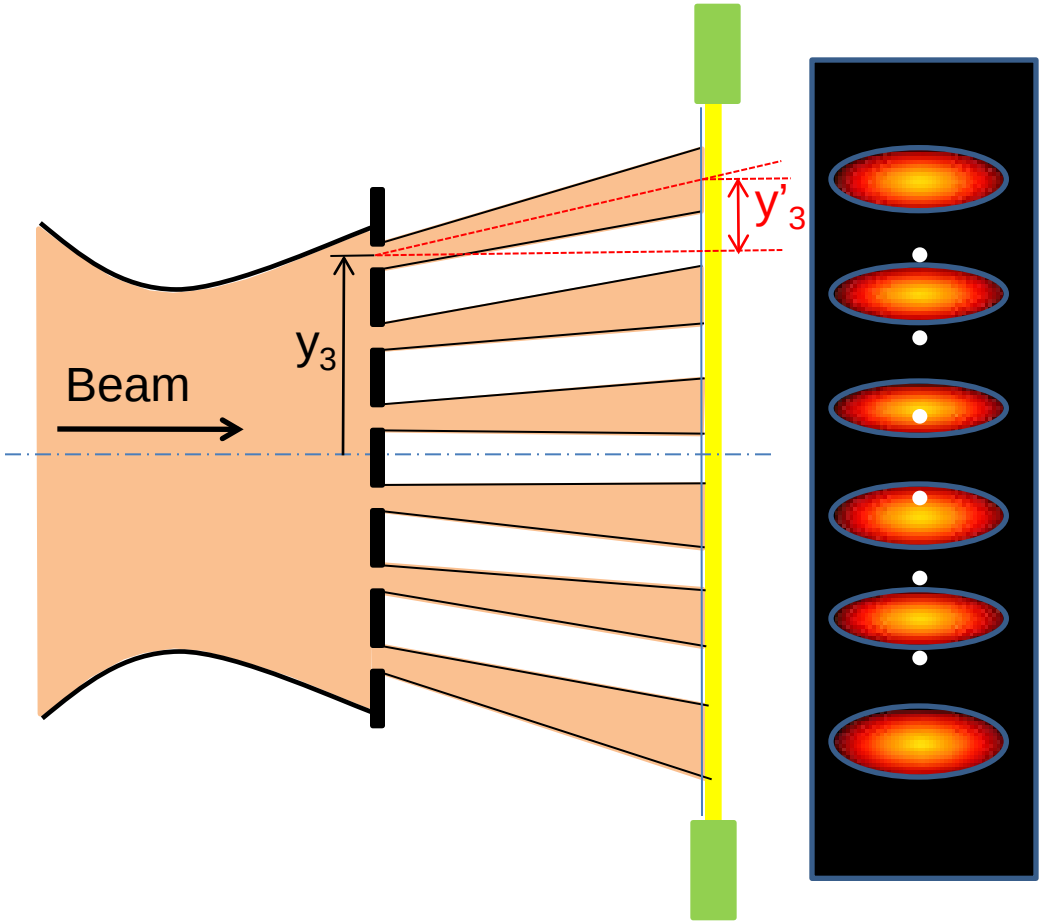

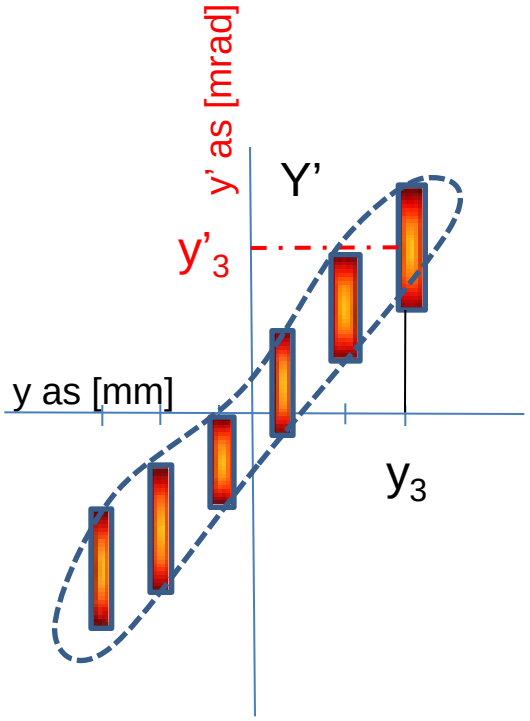

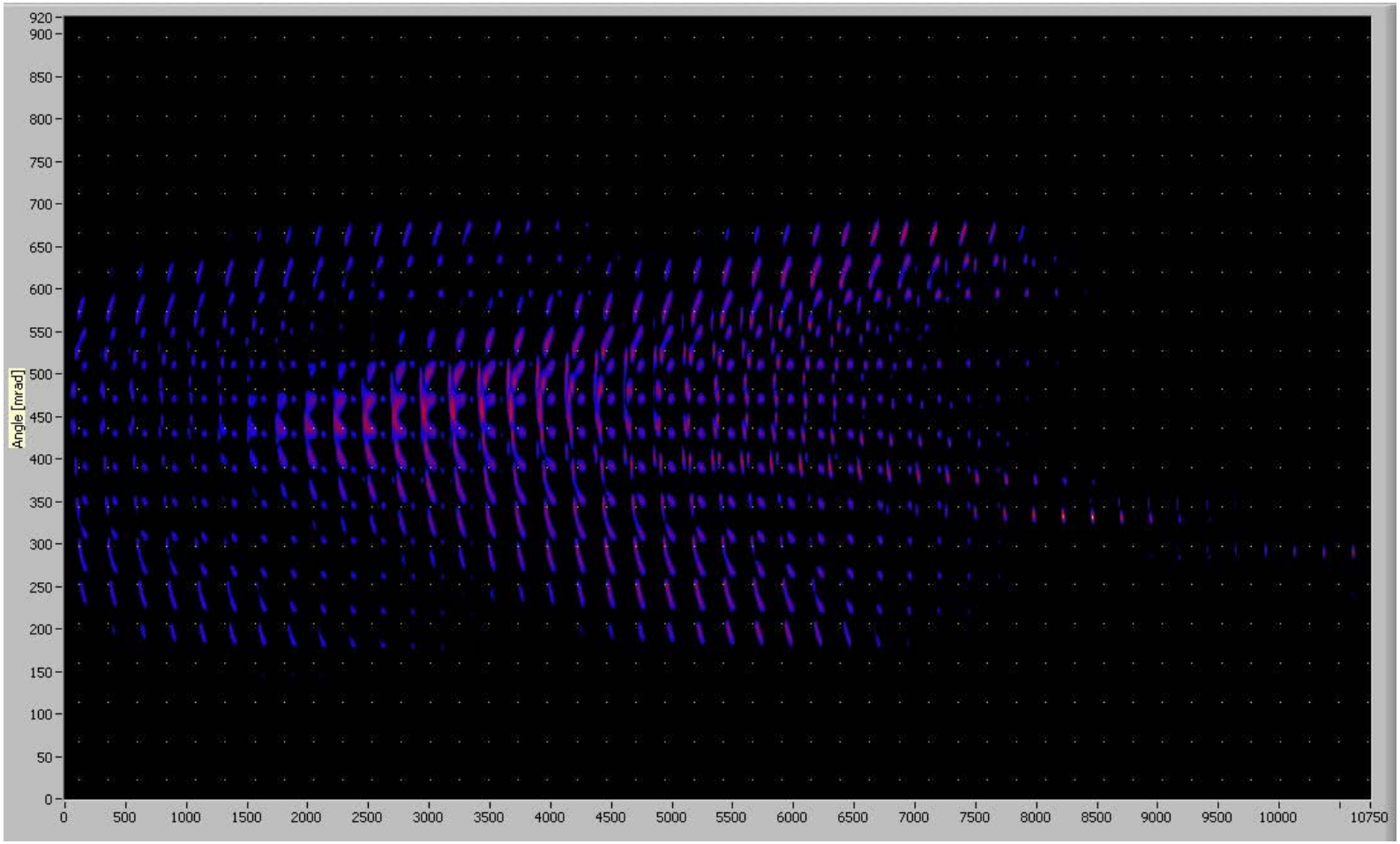
Angle [mrad]
920
900
850
800
750
700
650
600
550
500
450
400
350
300
250
200
150
100
50
0
0
500
1000
1500
2000
2500
3000
3500
4000
4500
5000
5500
6000
6500
7000
7500
8000
8500
9000
9500
10000
10750

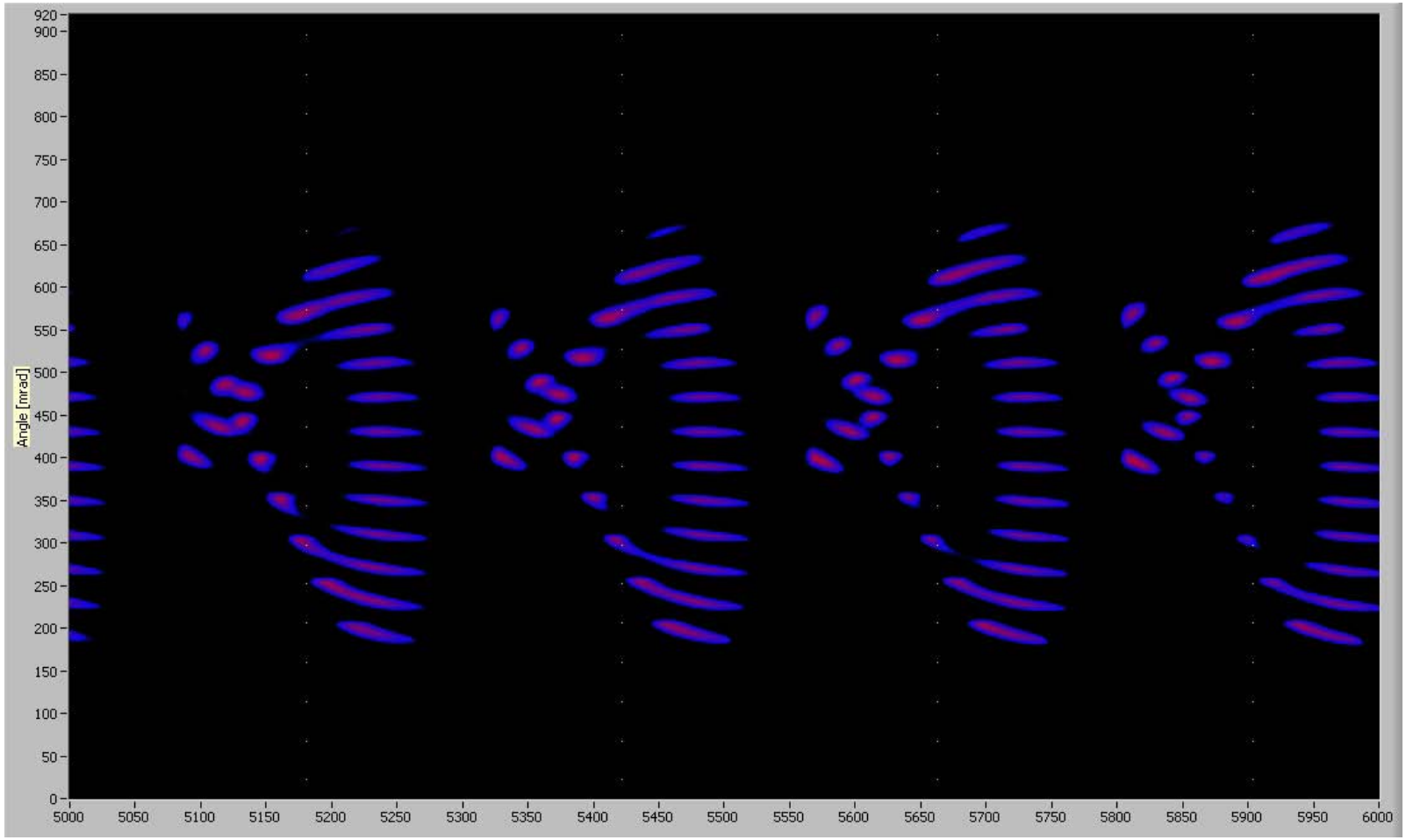
Angle [mrad]
920
900
850
800
750
700
650
600
550
500
450
400
350
300
250
200
150
100
50
0
5000
5050
5100
5150
5200
5250
5300
5350
5400
5450
5500
5550
5600
5650
5700
5750
5800
5850
5900
5950
6000

The emittances in the image plane

group 1

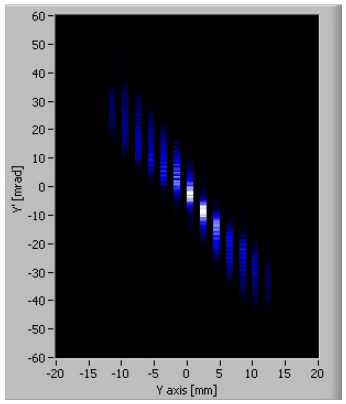

group 2,3

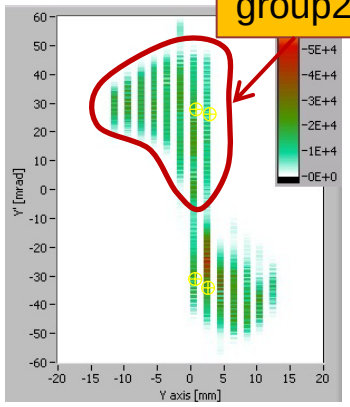

group 1,2,3

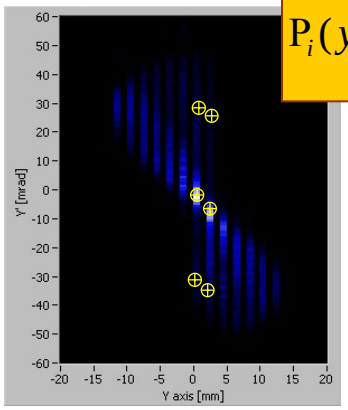

$$P_i(y,y') = \int_{x=-12mm\ x'=-60mrad}^{x=+12mm\ x'=+60mrad} \int \rho(x,x',y,y')_i dx dx'$$

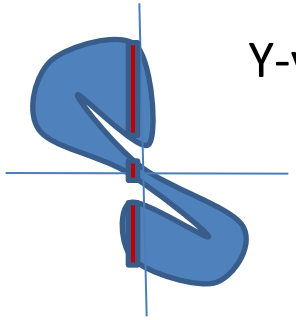

Y-y' projection's

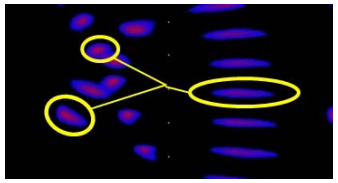

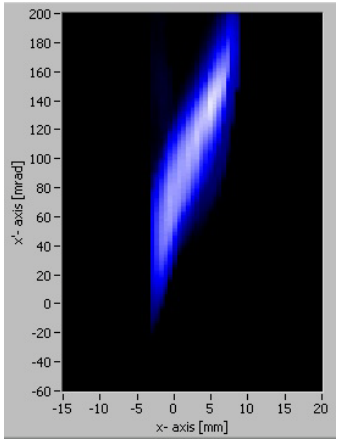

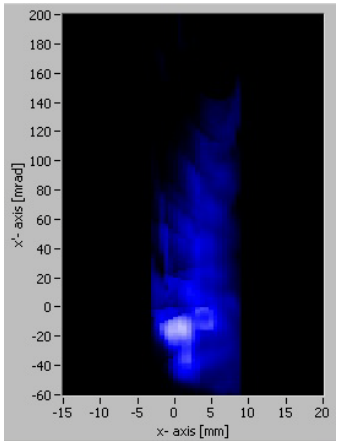

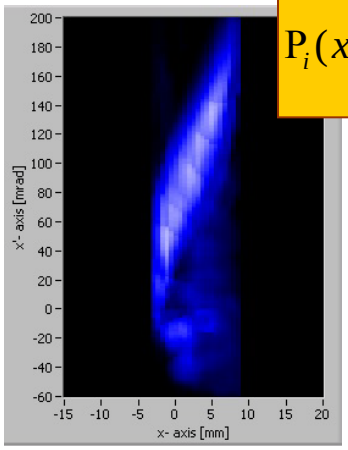

$$P_i(x,x') = \int_{y=-20mm\ y'=-20mrad}^{y=+20mm\ y'=+20mrad} \int \rho(x,x',y,y')_i dy dy'$$

X-x' projection